ICASSP 2023 - 2023 IEEE International Conference on Acoustics, Speech and Signal Processing (ICASSP) | 978-1-7281-6327-7/23/$31.00 ©2023 IEEE | DOI: 10.1109/ICASSP49357.2023.10095824

NEURALLY AUGMENTED STATE SPACE MODEL FOR SIMULTANEOUS COMMUNICATION AND TRACKING WITH LOW COMPLEXITY RECEIVERS

Fernando Pedraza, Giuseppe Caire

Communications and Information Theory Group, Technical University of Berlin, Berlin, Germany

ABSTRACT

In this paper, we propose an integrated sensing and communications (ISAC) system where a base station (BS) equipped with an antenna array and a co-located radar receiver transmits data packets while simultaneously tracking the position of users. We restrict our attention to the simplest hardware architecture, where the beamforming array can generate beams from a discrete codebook and the receiver is equipped with a single analog to digital converter, thereby allowing for scalar-only measurements where angular information is lost. Under such restrictive constraints, the observation likelihoods are hard to model, which motivates us to learn them via neural networks. This learned likelihoods are then incorporated into a state space model where Bayesian filtering can be performed. We test our method in complicated road geometries and show that our tracker is capable of following high mobility users most of the time. Furthermore, when the track of a user is lost, it often takes only a few measurements until is is recovered, disposing of the need for time consuming beam alignment procedures.

***Index Terms*—** Integrated Sensing and Communication, Beam Tracking, HMM, Neural Augmentation

1. INTRODUCTION

Millimeter wave (mmWave) communications are a fundamental technology of next generation networks, enabling multi-Gbps data rates thanks to the vast amount of available bandwidth [1]. Unfortunately, mmWave channels present the challenge of large propagation losses, which must be compensated by use of highly directional transceivers [2]. Fast adaptation to the channel is thus required to prevent beams from becoming obsolete, especially in high mobility scenarios [3]. In such conditions, the overhead associated with conventional pilot-based channel estimation schemes becomes prohibitively large [4].

Some proposed techniques to reduce the overhead involved include the design of active probing strategies [5, 6], which adaptively decide how to probe the channel, or the use of state space modeling techniques [7, 8, 3], where only a few uplink pilots are needed to update the estimate of the underlying state. The works [7] and [8] assume a priori statistical knowledge of the state evolution and observation models, and are therefore suitable for conventional model-based state space tracking approaches such as extended Kalman and particle filters. Differently, [3] assumes that knowledge of the state evolution model is unavailable and uses deep learning methods to obtain an approximation, while the rest of the processing remains model-based. Approaches of this type tend to perform better than purely data-driven methods since domain knowledge is incorporated in the algorithm architecture [9].

An alternative solution is to consider an ISAC system where the BS is complemented by a co-located radar receiver able to process the echoes of the information bearing transmitted signals [4, 10, 11]. Those techniques eliminate the need for active feedback and often yield measurements that are highly informative of the underlying channel. On the other hand, they tend to rely on costly receiver designs, either due to the large energy consumption required to sample high dimensional wideband signals [4, 10] or complicated radio frequency processing architectures [11].

In this paper, we consider an orthogonal frequency division multiplexing (OFDM)-based ISAC system with the simplest receiver architecture, corresponding to a single analog to digital converter and a finite set of available beams, thereby alleviating hardware design. Under this setup, measurements provide very limited information about the channel state. As a consequence, we propose to tackle the beam tracking problem with a neurally augmented hidden Markov model (HMM) filter that, similar to [3], replaces the unknown components with learned counterparts. Our system is therefore capable of performing beam tracking without the need for uplink pilots, while keeping hardware complexity and energy consumption to a minimum.

2. SYSTEM MODEL

Our studied setup consists of a mmWave downlink scenario where a BS, equipped with N_{tx} antennas and a co-located radar receiver with N_{rx} antennas, communicates with a user equipment (UE) as it moves within its coverage area. The

This work was partially supported by BMBF Germany in the program of "Souverän. Digital. Vernetzt." Joint Project 6G-RIC (Project IDs 16KISK030) and DFG, Grant agreement number KR 3517/11-1.

goal of the radar receiver is to predict the state of the channel such that the BS can choose an appropriate beam. Moreover, in order to simplify hardware implementation, we constrain the number of receiving chains to one and let BS and receiver use only beams from a finite codebook.

2.1. Channel model

We consider the two-way mmWave radar channel model [2]

$$\mathbf{H}(t,\tau)=\sum_{p=0}^{P} h_p \mathbf{b}(\phi_p)\mathbf{a}^{\mathsf{H}}(\theta_p)\delta(t-\tau_p)e^{j2\pi\nu_p t}, \quad (1)$$

consisting of a line of sight (LOS) path and P non-LOS (NLOS) paths, and where $(h_p,\phi_p,\theta_p,\tau_p,\nu_p)$ represent respectively the channel coefficient, angle of arrival (AoA), angle of departure (AoD), delay and Doppler associated with the p-th path. Focusing on uniform linear arrays (ULA) both at the transmitter and the radar receiver, the array response vectors $\mathbf{a}(\theta)$ and $\mathbf{b}(\phi)$ are given by

$$\begin{aligned}\left[\mathbf{a}(\theta)\right]_i &= e^{j\pi(i-1)\sin(\theta)} \qquad i\in 1,\dots,N_{\text{tx}}\\ \left[\mathbf{b}(\phi)\right]_i &= e^{j\pi(i-1)\sin(\phi)} \qquad i\in 1,\dots,N_{\text{rx}}.\end{aligned} \quad (2)$$

The channel coefficient for the two-way LOS path[1] is given by the point target radar range equation [12], as commonly assumed in the ISAC literature (e.g. [4, 13]), i.e.

$$|h_0|^2=\frac{\lambda^2\sigma_{\text{rcs}}}{(4\pi)^3 d^4}, \quad (3)$$

where λ is the wavelength at the carrier frequency, σ_{rcs} the radar cross section and d the distance to the UE.

2.2. Signal model

We choose OFDM since it is one of the standardized waveforms in mmWave communications [1] and because of its good properties as a sensing waveform [14]. The transmitted signal in the baseband is given by

$$\sum_{n=0}^{N-1}\sum_{m=1}^{M-1} x[n,m]\text{rect}\left(\frac{t-nT_0}{T_0}\right)e^{j2\pi m\Delta f(t-T_{\text{cp}}-nT_0)}, \quad (4)$$

where $x[n,m]$ is a frame of data symbols modulated over M subcarriers during N OFDM symbols, with average transmitted power $P_{\text{tx}}=\mathbb{E}[|x[n,m]|^2]$. The subcarrier spacing is denoted by Δf, the cyclic prefix by T_{cp}, and the symbol duration (including cyclic prefix) by T_0.

[1] We consider only the backscattering channel since the downlink and uplink channels depend on the transceiver characteristics of the UE (e.g. antenna architecture, beamforming strategy), which is not the focus of this paper.

At the l-th frame, the BS decides on a transmit beamforming vector $\mathbf{f}_l\in\mathcal{F}$ and the radar receiver on a combining vector $\mathbf{u}_l\in\mathcal{U}$ for the backscattered signal, where $\mathcal{F}$ and $\mathcal{U}$ are the finite transmit and receive codebooks respectively. After FFT and cyclic prefix removal, the signal at the receiver is given by (see [13])

$$\begin{aligned}&r_l[n,m]\\ &=\sum_{p=0}^{P} h'_{p,l}e^{j2\pi(nT_0\nu_{p,l}-m\Delta f\tau_{p,l})}x_l[n,m]+w[n,m]\\ &\approx h'_{p_l^*,l}e^{j2\pi(nT_0\nu_{p_l^*,l}-m\Delta f\tau_{p_l^*,l})}x_l[n,m]+w[n,m], \quad (5)\end{aligned}$$

where $w[n,m]$ is additive white gaussian noise (AWGN), and we have defined the combined channel coefficient $h'_{p,l}\triangleq h_{p,l}\mathbf{u}_l^{\mathsf{H}}\mathbf{b}(\phi_{p,l})\mathbf{a}^{\mathsf{H}}(\theta_{p,l})\mathbf{f}_l$ and $p_l^*\triangleq\arg\max_p|h'_{p,l}|$. The approximation follows from the assumption that $\mathbf{f}_l$ and $\mathbf{u}_l$ generate narrow beams and the AoAs and AoDs are not too closely spaced, such that at most one path can produce a received signal that is non-negligible with respect to the noise.

Given the received signal model in (5), we can obtain the maximum likelihood estimate of $(h'_{p_l^*,l},\tau_{p_l^*,l},\nu_{p_l^*l})$ as [15]

$$\begin{aligned}&(\hat{\tau}_{p_l^*,l},\hat{\nu}_{p_l^*,l})\\ &\quad=\arg\max_{\tau,\nu}\left|\sum_{n,m} r_l[n,m]x_l^{\text{c}}[n,m]e^{-j2\pi(nT_0\nu-m\Delta f\tau)}\right|, \quad (6)\end{aligned}$$

$$\hat{h}'_{p_l^*,l}=\frac{\sum_{n,m} r_l[n,m]x_l^{\text{c}}[n,m]e^{-j2\pi(nT_0\hat{\nu}_{p_l^*,l}-m\Delta f\hat{\tau}_{p_l^*,l})}}{\sum_{n,m}|x_l[n,m]|^2}, \quad (7)$$

where $(\cdot)^{\text{c}}$ indicates the complex conjugate.

3. LEARNED HMM FOR BEAM SELECTION

In this section, we propose a strategy to choose the beamforming vectors to be used at each frame given the estimated magnitudes in (6) and (7). For ease of exposition, we will treat the case $N_{\text{tx}}=N_{\text{rx}}$ and $\mathcal{U}=\mathcal{F}$. Furthermore, we focus on tracking the LOS path, for which the AoA and AoD coincide, and therefore select the same beamforming vector for transmission and reception at each frame. Extensions to different transmit-receive architectures and NLOS paths are feasible but out of the scope of this paper.

Under the system model presented in section 2, tracking the best beam can be seen as a Bayesian filtering problem where the index $Z_l\in\{1,\dots,|\mathcal{F}|\}$ of the best beam is a latent variable in a finite state space and the observations are defined by $\mathbf{y}_l=(\hat{h}'_{p_l^*,l},\hat{\tau}_{p_l^*,l},\hat{\nu}_{p_l^*l})$. If the sequence of best beams satisfies the Markov property, then it is well known [16] that

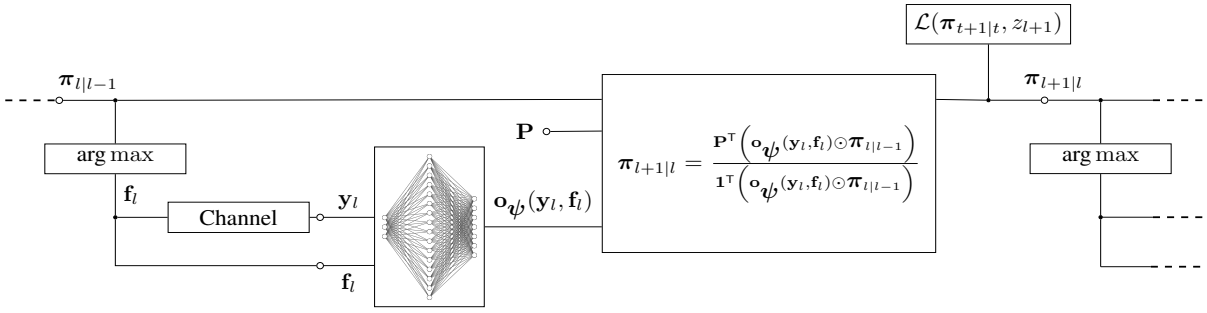

Fig. 1. Block diagram representing the learning and inference procedures of the proposed neurally augmented HMM filter. In the figure, white filled circles indicate points in which backpropagation is interrupted.

the optimal filter recursively computes the posterior

$$\begin{aligned}\boldsymbol{\pi}_{l+1|l} &\triangleq [\mathbb{P}(Z_{l+1} = 1 \mid \mathbf{y}_1^l), \dots \mathbb{P}(Z_{l+1} = |\mathcal{F}| \mid \mathbf{y}_1^l)]^\intercal \\ &= \frac{\mathbf{P}^\intercal\left(\mathbf{o}(\mathbf{y}_l, \mathbf{f}_l) \odot \boldsymbol{\pi}_{l|l-1}\right)}{\mathbf{1}^\intercal\left(\mathbf{o}(\mathbf{y}_l, \mathbf{f}_l) \odot \boldsymbol{\pi}_{l|l-1}\right)}, \end{aligned} \tag{8}$$

where $\mathbf{y}_1^l$ is shorthand for $(\mathbf{y}_1, \dots, \mathbf{y}_l)$, $\odot$ is the Hadamard (elementwise) product of two vectors, $\mathbb{P}(A)$ indicates the probability of event A, $\mathbf{1}$ is a vector of all ones, and $\mathbf{o}(\mathbf{y}_l, \mathbf{f}_l)$ is a vector whose i-th component corresponds to the likelihood of observing $\mathbf{y}_l$ given that the true state is $Z_l = i$ and beamforming vector $\mathbf{f}_l$ was used. Finally, $\mathbf{P}$ is a stochastic matrix that contains the transition probabilities for the latent variable Z_l, such that $[\mathbf{P}]_{i,j} = \mathbb{P}(Z_{l+1} = j \mid Z_l = i)$. In most cases, the sequence of optimal beam indices $\{Z_l\}$ has longer temporal dependencies and therefore does not satisfy the Markov property. However, as already noted in [3], modeling the dynamics as Markovian helps with tractability while still providing good performance in general mobility patterns. We assume that tracking starts after a successful initial beam alignment phase (e.g. by applying the method in [5] or [6]), and therefore initialize $\boldsymbol{\pi}_{1|0}$ to the degenerate distribution that concentrates all its mass at the optimal beam index.

In general, the transition matrix $\mathbf{P}$ is not known in advance and the function $\mathbf{o}(\mathbf{y}_l, \mathbf{f}_l)$ is hard to evaluate due to the uncertainty in the AoA/AoD, since a given value of Z_l corresponds to a dense set of angles, and therefore the beamforming gain is not fully specified by the state. As a solution, we propose in this paper to learn $\mathbf{P}$ and $\mathbf{o}(\mathbf{y}_l, \mathbf{f}_l)$ from examples via stochastic optimization. In particular, we let every coefficient of $\mathbf{P}$ be a trainable parameter and replace the mapping $\mathbf{o}$ with an approximated representation $\mathbf{o}_{\boldsymbol{\psi}}$ parametrized by a neural network with weights $\boldsymbol{\psi}$.

3.1. Model learning

In order to learn the transition matrix $\mathbf{P}$ and the mapping $\mathbf{o}_{\boldsymbol{\psi}}$, the system is fed with many simulated trajectories and trained end-to-end to minimize the cross entropy loss $\mathcal{L}(\boldsymbol{\pi}_{l|l-1}, z_l) \triangleq -\log\left[\boldsymbol{\pi}_{l|l-1}\right]_{z_l}$ between the predicted posterior $\boldsymbol{\pi}_{l|l-1}$ and the ground truth latent state z_l for each frame of each trajectory. A block diagram illustrating the process for a given frame is shown in Figure 1. The tracker finds the beam index that maximizes the approximate posterior $\boldsymbol{\pi}_{l|l-1}$ and chooses that beam to transmit information and receive a measurement. The beam index and the measurement are input to a fully connected neural network that approximates the likelihood function $\mathbf{o}(\mathbf{y}_l, \mathbf{f}_l)$. Finally, the posterior is updated using (8) and the loss is evaluated. After a batch of trajectories is processed, the coefficients of $\mathbf{P}$ and the parameters $\boldsymbol{\psi}$ are updated by performing a stochastic gradient descent step on the loss averaged over frames and trajectories. Following the gradient step, the rows of $\mathbf{P}$ need to be normalized to ensure it remains a stochastic matrix.

Since the dynamic aspect of the filter is implemented in the recursive update (8), gradient propagation is stopped in the locations indicated with white circles in Figure 1. This results in more stable gradient updates, and a better resemblance to model based filtering, where the likelihood computation should not be influenced by previous predictions. Furthermore, to facilitate early stages of training, we apply scheduled sampling [17], whereby at first we provide the optimal beamforming actions in order to obtain meaningful sequences of observations, to then gradually force the system to make its own decisions such that it can learn to recover from erroneous actions.

After extensive hyperparameter search, the chosen architecture for $\mathbf{o}_{\boldsymbol{\psi}}$ is a three layer fully connected neural network, where each hidden layer contains 1024 units with layer normalization and ReLU activations. The output layer has dimension $|\mathcal{F}|$ and uses softplus activations to ensure that the predicted likelihoods are strictly positive. The system is trained using the Adam optimizer [18] with a fixed learning rate of 0.003 and 1000 batches of 32 trajectories.

4. NUMERICAL RESULTS

We evaluate our approach on 200 trajectories with $50\,\mathrm{ms}$ interval between measurements generated following the same

Table 1. System parameters

$N = 14$	$M = 1024$
$N_{\text{tx}} = N_{\text{rx}} = \lvert\mathcal{U}\rvert = \lvert\mathcal{F}\rvert = 64$	$\sigma_{\text{rcs}} = 20\,\text{dBsm}$
$f_{\text{c}} = 60\,\text{GHz}$	$\Delta f = 1\,\text{MHz}$
$d_{\max} = 100\,\text{m}$	$v_{\max} = 30\,\text{m/s}$
Noise PSD: $N_0 = -174\,\text{dBm/Hz}$	$P_{\text{tx}} = 25\,\text{mW}$

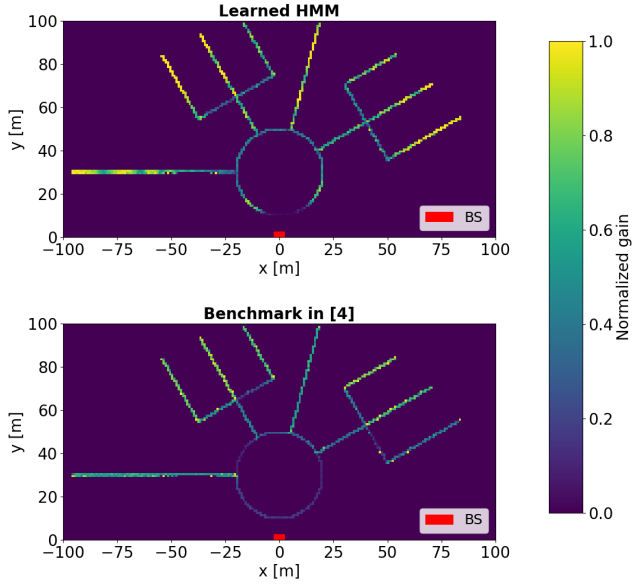

Fig. 2. Normalized transmit beamforming gain as a function of the position, averaged over 200 trajectories.

method as in [11], omitted here due to space limitations. Codebooks entries correspond to the columns of the DFT matrix to facilitate hardware implementation. The values used for all the relevant system parameters are specified in Table 1.

We compare the performance of our system to the benchmark in [4] that assumes sampling at every antenna, allows for continuous control of the pointing direction and considers a perfectly known observation model. As a performance metric, we define the normalized transmit beamforming gain, given at the l-th frame as

$$g_{\text{tx,l}} \triangleq \frac{1}{N_{\text{tx}}} |\mathbf{a}_l^{\text{H}}(\theta)\mathbf{f}_l|^2, \tag{9}$$

which indicates the ratio between the gain obtained by the chosen beamformer and the upper bound attained when $\mathbf{f}_l = \frac{1}{\sqrt{N_{\text{tx}}}}\mathbf{a}(\theta)$.

In order to provide a fair performance evaluation, we partition the coverage area into $1\,\text{m}^2$ pixels and average the normalized transmit beamforming gain achieved at each of them, thereby averaging different velocities, accelerations, starting and ending points. The results for our learned HMM and the method in [4] are presented in Figure 2. It is clearly seen that, in spite of having a much more limited architecture, our method is capable of better tracking the moving user at almost all positions. Interestingly, due to the finiteness of the beam codebooks, some transitions can be observed in the figure, suggesting that in many cases the loss in performance is due to hardware restrictions rather than algorithmic. Such gaps could be filled by considering larger codebooks with overlapping beams at the expense of higher processing power and training time.

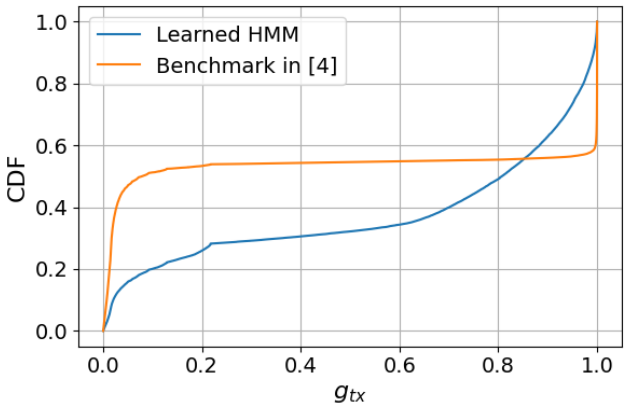

Fig. 3. Empirical CDF of the normalized transmit beamforming gain for our method and the benchmark in [4].

To better understand the performance of both methods, we continue by presenting the empirical CDF of the normalized transmit beamforming gain in Figure 3. Noticeably, the CDF of the benchmark in [4] shows two main modes, namely perfect tracking and lost track. Contrarily, our approach reveals a smooth transition, seemingly indicating that situations of permanent lost track are uncommon. We remark that our tracker achieves optimal normalized beamforming gain only marginally as a result of its much simpler hardware architecture where the beam codebooks are finite dimensional.

5. CONCLUSIONS AND FUTURE WORK

We have introduced a method for ISAC based beam tracking that relies on a simple receiver architecture. By combining model-based state space filtering techniques with data-driven function approximation, our tracker is able to outperform state of the art approaches while remaining cost efficient. Studying how performance is affected with codebook size, hierarchical codebooks or different beam patterns is an interesting topic for further research.

6. REFERENCES

[1] Xiong Wang, Linghe Kong, Fanxin Kong, Fudong Qiu, Mingyu Xia, Shlomi Arnon, and Guihai Chen, "Millimeter wave communication: A comprehensive survey," *IEEE Communications Surveys & Tutorials*, vol. 20, no. 3, pp. 1616–1653, 2018.

[2] J. Andrew Zhang, Fan Liu, Christos Masouros, Robert W. Heath, Zhiyong Feng, Le Zheng, and Athina Petropulu, "An overview of signal processing techniques for joint communication and radar sensing," *IEEE Journal of Selected Topics in Signal Processing*, vol. 15, no. 6, pp. 1295–1315, 2021.

[3] Muddassar Hussain and Nicolò Michelusi, "Learning and adaptation for millimeter-wave beam tracking and training: A dual timescale variational framework," *IEEE Journal on Selected Areas in Communications*, vol. 40, no. 1, pp. 37–53, 2022.

[4] Fan Liu and Christos Masouros, "A tutorial on joint radar and communication transmission for vehicular networks—part iii: Predictive beamforming without state models," *IEEE Communications Letters*, vol. 25, no. 2, pp. 332–336, 2021.

[5] Sung-En Chiu, Nancy Ronquillo, and Tara Javidi, "Active learning and csi acquisition for mmwave initial alignment," *IEEE Journal on Selected Areas in Communications*, vol. 37, no. 11, pp. 2474–2489, 2019.

[6] Foad Sohrabi, Tao Jiang, Wei Cui, and Wei Yu, "Active sensing for communications by learning," *IEEE Journal on Selected Areas in Communications*, vol. 40, no. 6, pp. 1780–1794, 2022.

[7] Jaechan Lim, Hyung-Min Park, and Daehyoung Hong, "Beam tracking under highly nonlinear mobile millimeter-wave channel," *IEEE Communications Letters*, vol. 23, no. 3, pp. 450–453, 2019.

[8] Seong-Hwan Hyun, Jiho Song, Keunwoo Kim, Jong-Ho Lee, and Seong-Cheol Kim, "Adaptive beam design for v2i communications using vehicle tracking with extended kalman filter," *IEEE Transactions on Vehicular Technology*, vol. 71, no. 1, pp. 489–502, 2022.

[9] Guy Revach, Nir Shlezinger, Xiaoyong Ni, Adrià López Escoriza, Ruud J. G. van Sloun, and Yonina C. Eldar, "Kalmannet: Neural network aided kalman filtering for partially known dynamics," *IEEE Transactions on Signal Processing*, vol. 70, pp. 1532–1547, 2022.

[10] Weijie Yuan, Fan Liu, Christos Masouros, Jinhong Yuan, Derrick Wing Kwan Ng, and Nuria González-Prelcic, "Bayesian predictive beamforming for vehicular networks: A low-overhead joint radar-communication approach," *IEEE Transactions on Wireless Communications*, vol. 20, no. 3, pp. 1442–1456, 2021.

[11] Fernando Pedraza, Saeid K. Dehkordi, Mari Kobayashi, and Giuseppe Caire, "Simultaneous communication and tracking in arbitrary trajectories via beam-space processing," in *2022 IEEE 12th Sensor Array and Multichannel Signal Processing Workshop (SAM)*, 2022, pp. 236–240.

[12] Mark A Richards, *Fundamentals of radar signal processing*, Tata McGraw-Hill Education, 2005.

[13] Christian Sturm and Werner Wiesbeck, "Waveform design and signal processing aspects for fusion of wireless communications and radar sensing," *Proc. IEEE*, vol. 99, no. 7, pp. 1236–1259, 2011.

[14] Lorenzo Gaudio, Mari Kobayashi, Bjorn Bissinger, and Giuseppe Caire, "Performance analysis of joint radar and communication using ofdm and otfs," in *2019 IEEE International Conference on Communications Workshops (ICC Workshops)*, 2019, pp. 1–6.

[15] Fernando Pedraza, Mari Kobayashi, and Giuseppe Caire, "Beam refinement and user state acquisition via integrated sensing and communication with ofdm," in *2021 IEEE 22nd International Workshop on Signal Processing Advances in Wireless Communications (SPAWC)*, 2021, pp. 476–480.

[16] V. Krishnamurthy, *Partially Observed Markov Decision Processes*, Partially Observed Markov Decision Processes: From Filtering to Controlled Sensing. Cambridge University Press, 2016.

[17] Samy Bengio, Oriol Vinyals, Navdeep Jaitly, and Noam Shazeer, "Scheduled sampling for sequence prediction with recurrent neural networks," in *Proceedings of the 28th International Conference on Neural Information Processing Systems - Volume 1*, Cambridge, MA, USA, 2015, NIPS'15, p. 1171–1179, MIT Press.

[18] Diederik P. Kingma and Jimmy Ba, "Adam: A method for stochastic optimization," 2014.